PREDICTING THE FRACTURE CHARACTER OF POTENTIAL WEAK LAYERS IN PENETROMETER SIGNALS

James Floyer[1,*] and Bruce Jamieson[1,2]
[1]Department of Geoscience, [2]Department of Civil Engineering
University of Calgary, Calgary, AB, Canada

ABSTRACT: Digital penetrometers have been shown to provide reliable assessments of snow hardness with depth; however, extracting useful information from the signals relating to stability has proved to be challenging. A scheme for predicting the fracture character of potential weak layers from penetrometer signals is developed. When a two-group classification between *sudden* (Q1) and *other* fracture character groups is performed, potential failure layers are correctly classified 80% of the time. The variables offering the best discrimination between *sudden* and *other* categories are weak layer thickness, average force gradient above the weak layer and, interestingly, both the average and the maximum force gradient below the weak layer. By itself, the fracture character prediction scheme is of limited practical use, since it requires the depth of the potential failure interface to be identified. However, we discuss how a weak layer tracing algorithm could be used as the basis for an operational model to detect weak layers from penetrometer profiles. By using the weak layer detection model in conjunction with the fracture character prediction, rapid, automatic identification of critical weak layers becomes possible.

KEYWORDS: snow penetrometer, fracture character, snowpack stratigraphy, avalanche forecasting, snowpack properties, snow hardness

1. INTRODUCTION

Digital force-resistance penetrometers (e.g. Schneebeli and Johnson, 1998; Mackenzie and Payten, 2002) are able to make rapid measurements of snow hardness with depth; these measurements are useful for characterising snowpack stratigraphy at the measurement location (Johnson and Schneebeli, 1999; Pielmeier and Schneebeli, 2003). However, critical information for avalanche forecasting includes a determination of whether there is a weak layer (or layers) in the snowpack and if so, how reactive the weak layer is to loading by snowfall, rain, wind-blown snow or human-triggering. At present, manual snow observations are generally relied on to provide this information, using techniques that include analysing snow hardness, grain type and conducting (in)stability tests such as the rutschblock test or compression test (McClung and Schaerer, 2006, p.173).

Assessing the character of fractures identified in isolated-column tests has gained rapid acceptance over the last five to ten years as a good aid for determining critical weak layers in the snowpack. Birkeland and Johnson (1999) and Johnson and Birkeland (2002) presented the *shear quality* classification scheme (Q1, Q2, Q3), originally in association with the stuffblock test. This scheme has been adopted for use in the USA (Birkeland, 2004; Greene and others, 2004). Jamieson (1999) described a four-point system for recording the character of failures, which could be applied to compression and other snowpack tests. van Herwijnen and Jamieson (2005, 2007) modified Jamieson's scheme into the five-point *fracture character* classification scheme that is currently in use in Canada (CAA, 2007, p.40). Schweizer and Wiesinger (2001) presented a three-point scheme for rating the quality of rutschblock fractures (clean, partly clean, rough), which was later modified by Schweizer (2002) (smooth, rough, irregular). Schweitzer (2002) also presented a *release type* classification for rutschblock tests (whole block, part of block, edge of block). A similar classification to this is now in use by Canadian avalanche operations (CAA, 2007, p.33).

In this study, we attempt to relate the shape of the penetrometer signal at fracture interfaces to the fracture character associated with those fractures. A scheme is presented that allows penetrometer profile segments to be separated into the two broad classes of *sudden* and *other* fractures, which are the major categories of the fracture character scheme described by van Herwijinen and Jamieson (2007). This is achieved by first selecting suitable variables from the

* *Corresponding author address:*
James Floyer
Tel: 250-837-3253
Email: jafloyer@gmail.com

penetrometer signals using a univariate analysis and then developing a two-group discriminant model using the selected variables. We also explain how a recently proposed method for detecting weak layers in penetrometer profiles could be used in conjunction with this fracture character prediction scheme to allow the method to be applied where weak layers have not been pre-identified in the penetrometer profile.

2. PREDICTING FRACTURE CHARACTER

2.1 Method

Data for this study came from a set of compression tests and penetrometer profiles that were collected in close proximity to each other at a number of different sites during the winter of 2007-2008. In total, 78 penetrometer profiles and 56 compression test results were collected from 28 different site-days and 16 unique sites. For sites that were visited more than once on different days, care was taken to select a previously undisturbed site for the new set of measurements. In addition to the penetrometer profiles and compression tests, a manual snow profile was recorded at each site. The relative location of the measurements made at each site is shown in Figure 1.

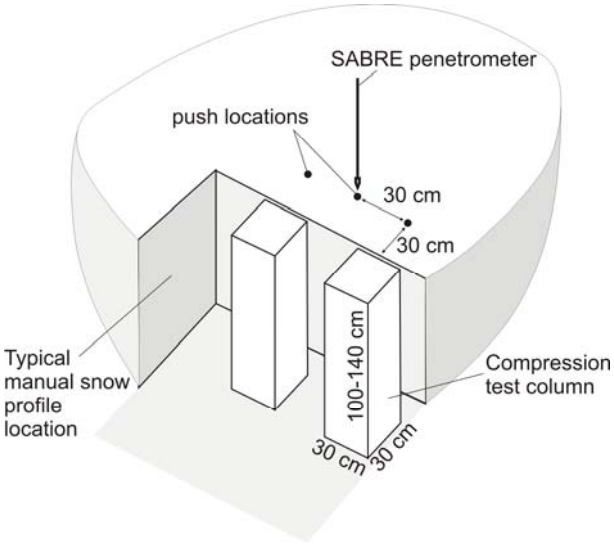

Figure 1: Schematic showing compression test geometry and penetrometer push locations.

The penetrometer profiles were collected using a modified (Floyer, 2008, p.56) SABRE penetrometer (Mackenzie and Payten, 2002) manufactured by Himachal Safety Systems. This instrument recorded force-resistance with depth at a frequency of 1000 Hz. It was manually driven, vertically through the snow, resulting in a variable depth interval between measurement points.

In a previous study (Floyer, 2008, p.81), it was shown that changes in the push velocity did not influence the force-resistance values in uniform snow provided that the instrument had reached a point of steady state deformation (attained within the first 6 cm during that study) and that the push velocity was kept within the velocity range of 30 to 100 cm s^{-1}. With the exception of near-surface measurements, velocities used in this study were found to be within this range. For this reason, and to address the steady-state issue, near-surface fractures, to a depth of approximately 20 cm, were not considered in this analysis.

Two standard compression tests were performed at each site (CAA, 2007, p.32; Greene and others, 2004, p.45). Depths to fracture interfaces were measured to the nearest 1 cm. The fracture character of each fracture was assessed for each fracture. During most of the tests, two people, an operator and an observer, agreed on each fracture character determination, reducing the subjectivity of determining the fracture character.

In order to prevent the same fracture being included in the analysis more than once, only one penetrometer push was interpreted from each site-day investigated. There were between one and seven fractures identified in each compression test. Sometimes, fractures only appeared in one compression test and not the other. When this occurred, fractures that were present in either test column were deemed to be interpretable in the penetrometer profile.

Fractures in low resistance snow could not be interpreted due to the inability of the SABRE penetrometer to reliably distinguish hardness differences in snow of this type. Fractures that occurred in fist hardness and in some cases, 4-finger hardness snow were impossible to identify in the penetrometer signals and were excluded from the analysis.

2.2 Results

In total, 83 weak layers/interfaces were identified in the penetrometer signals. Of these, 41 were resistant planar fractures, 20 were *sudden collapse*, 14 were *non-planar breaks*, seven were *sudden planar*, and 1 was a *progressive compression*. Due to the low numbers of *sudden planar* and *progressive compression* fractures, it was decided to combine the classes into *sudden*

fractures (*sudden collapse* and *sudden planar*) and *others* (*resistant planar*, *non-planar breaks* and *progressive compression*); this grouping reflects the higher incidence of skier-triggered avalanches associated with *sudden* fractures (van Herwijnen and Jamieson, 2007).

Two examples of interpreted penetrometer pushes are shown in Figure 2, with the corresponding compression test results indicated at each fracture location. Weak layers (with thickness) are shown with a horizontal grey bar, with the top of the bar representing the top of the weak layer and the bottom of the bar representing the bottom of the weak layer. Interfaces (with no thickness) are shown with a dotted grey line.

2.3 Univariate analysis

A number of variables describing the penetrometer signal associated with the weak layer or interface identified by the compression test fractures were considered. These variables are listed in Table 1. In the variable names given, an "A" in the name means that the parameter was assessed above the top of the weak layer, over a distance in mm given by the proceeding number. A "B" in the name means that the parameter was assessed below the bottom of the weak layer, again over the given distance in mm.

In Table 1, *t* and *p* statistics are shown for group separation between the *sudden* and *other* groups for each variable. A positive *t* value indicates the mean value of that variable for the *other* group is higher than the *sudden* group. Variables with significant results at α=0.05 are indicated in bold.

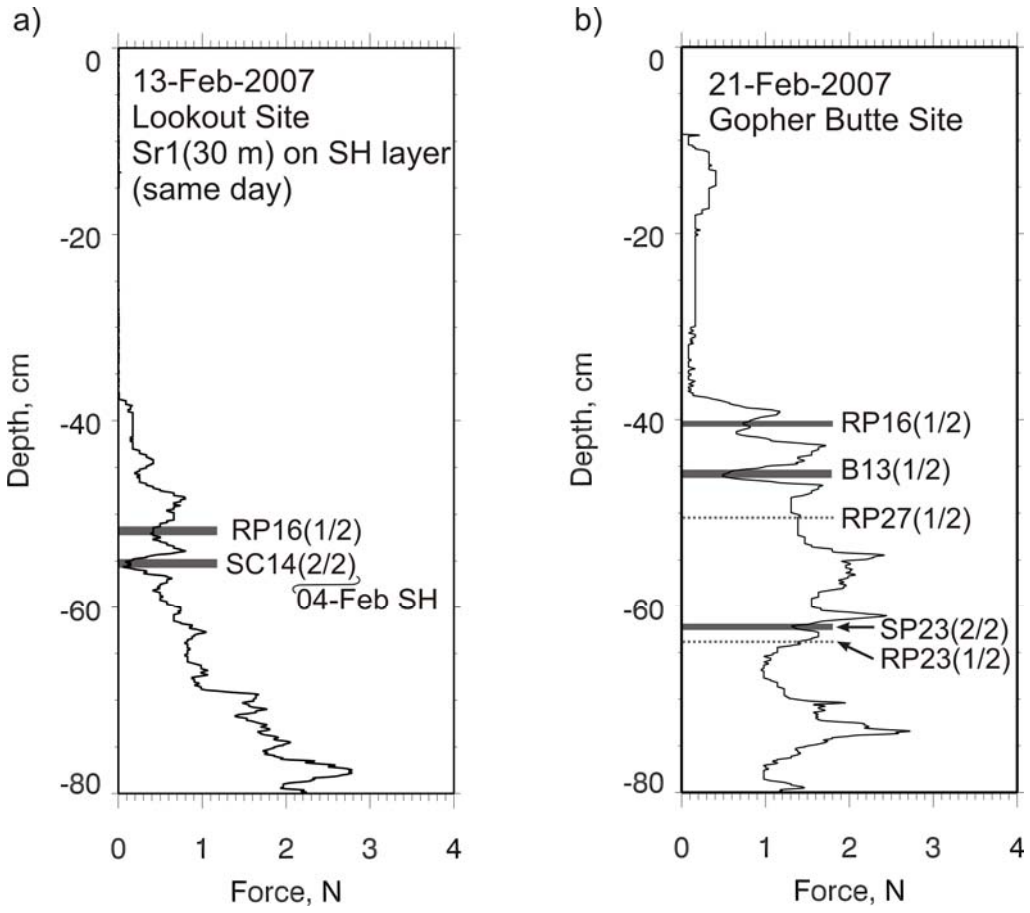

Figure 2: Compression test fracture locations interpreted onto four penetrometer profiles. Weak layers (with thickness) shown with a dark grey bar; interfaces (with no thickness) shown with a grey dotted line. SP = sudden planar; SC = sudden collapse; RP = resistant planar; PC = progressive compression; B = non-planar break. Numbers in parentheses represent the number of compression tests in which this result was seen out of a total number conducted at that site. Local avalanche observations noted: a) Lookout site, skier remote at 30 m; b) Gopher Butte site, no avalanche observations.

Table 1: Variables used in the fracture character comparison analysis. Bold type indicates significant mean differences between the *sudden* and *other* groups at α=0.05.

Variable name	Units	*t*	*p*	Description
WL_D	cm	**2.70**	**0.009**	Weak layer depth
WL_Thick	mm	**-4.84**	**<0.001**	Weak layer thickness
WL_H	N	-1.36	0.177	Mean weak layer hardness
Ratio_Slab_WL_10A		-1.69	0.095	Ratio of mean slab hardness to mean weak layer hardness. Mean slab hardness calculated over 10, 20, 50, 100 and 200mm above the top of the weak layer.
Ratio_Slab_WL_20A		0.74	0.464	
Ratio_Slab_WL_50A		1.16	0.248	
Ratio_Slab_WL_100A		1.19	0.238	
Ratio_Slab_WL_200A		1.11	0.271	
Avg_Grad_1A	N mm^{-1}	1.52	0.132	Average hardness gradient over a distance of 1, 5, 10, 20 and 50 mm above the top of the weak layer.
Avg_Grad_5A		**2.47**	**0.016**	
Avg_Grad_10A		**3.03**	**0.003**	
Avg_Grad_20A		**3.14**	**0.002**	
Avg_Grad_50A		**3.18**	**0.002**	
Avg_Grad_1B	N mm^{-1}	-1.94	0.056	Average hardness gradient over a distance of 1, 5, 10, 20 and 50 mm below the bottom of the weak layer.
Avg_Grad_5B		**-2.09**	**0.039**	
Avg_Grad_10B		**-1.99**	**0.050**	
Avg_Grad_20B		**-2.44**	**0.017**	
Avg_Grad_50B		**-2.31**	**0.024**	
Max_Grad_1A	N mm^{-1}	**-2.14**	**0.035**	Maximum hardness gradient over a distance of 1, 5, 10, 20 and 50 mm above the top of the weak layer.
Max_Grad_5A		**-2.30**	**0.024**	
Max_Grad_10A		**-2.23**	**0.028**	
Max_Grad_20A		**-2.76**	**0.007**	
Max_Grad_50A		**-2.11**	**0.038**	
Max_Grad_1B	N mm^{-1}	**-3.53**	**0.001**	Maximum hardness gradient over a distance of 1, 5, 10, 20 and 50 mm above the top of the weak layer respectively.
Max_Grad_5B		**-3.79**	**<0.001**	
Max_Grad_10B		**-2.87**	**0.005**	
Max_Grad_20B		**-3.22**	**0.002**	
Max_Grad_50B		**-3.38**	**0.001**	

The large number of variables tested reflects uncertainty over how far from the weak layer some of the parameters should be measured. For the ratio of slab hardness to weak layer hardness, none of the measurement distances were significant for group separation, which was surprising and a result that warrants further investigation. For the average hardness gradient above and below the weak layer, the optimum distance, based initially on the lowest *p* value and subsequently on the *t* value with the highest magnitude, was 20 mm from the weak layer interface. For the maximum hardness gradient (the magnitude of the gradient was used for this variable, which explains the negative *t* values for both above and below the weak layer), the optimum distance above the weak layer was 20 mm, whereas for below the weak layer, the optimum distance was 5 mm.

The following variables were selected for the discriminant model: WL_Thick, Avg_Grad_20A, Avg_Grad_20B, Max_Grad_20A, and MaxGrad_5B. Weak layer depth was not selected, since the overlap of the interquartile range of weak layer depth for the *sudden* and *other* groups (Figure 3) shows that, while the mean value differs significantly between the two groups, the variable does not offer good group discrimination. In order to reduce collinearity, only the optimum distance variable from each group of gradient variables was selected, despite the fact that more than one variable was shown to be significant for group separation.

2.4 Discriminant analysis

A linear discriminant analysis (e.g. Manly, 1994, p.107) was performed using the variables selected from the univariate analysis above. Discriminant analysis seeks to find a linear combination of the predictor variables, $Z = A_1 X_1 + A_2 X_2 + \ldots + A_m X_m$, that exhibits the largest difference between group means relative to the within-group variance.

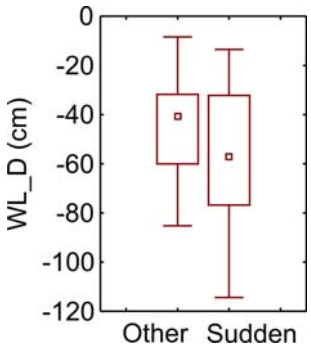

Figure 3: Box plot of the interquartile range of weak layer depth for sudden and other groups. Box shows the 25%-75% range; whiskers show the non-outlier min-max and the small square shows the median value.

For discriminant analysis, it is advantageous to use group sizes that are approximately equal. This ensures that the a-priori probability of predicting *sudden* group membership is the same as predicting *other* group membership, and should result in parity between classification rates for the two groups. Equal group size was achieved by eliminating records from the *other* category using a random number generator. Out of an original 110 data points, only 54 were selected: 27 for each group. Due to the small group sizes, a leave-one-out cross-validation approach was used for independent validation of the model.

Group separation is indicated using Wilks' Lambda (Wilkinson, 1990), which is the ratio of within-groups sums of squares to the total sums of squares. It takes a value between 0 and 1 with a value near 0 indicating that the (multivariate) group means are different and a value near 1 indicating that group means are the same. For this analysis, Wilks' Lambda=0.43, which is encouraging, as it indicates reasonable group separation between *sudden* and *other* fractures. The associated F statistic is 5.4, with p=0.007, which indicates that group separation is significant at the α=0.05 level.

The standardised discriminant function weights and the factor structure coefficients (loadings) are shown in Table 2. The discriminant function weights denote the unique (partial) contribution of each variable to the discriminant functions, while the structure coefficients denote the simple correlations between the variables and the functions; therefore, the structure coefficients are more appropriate for substantive interpretations of the functions (StatSoft, 2007). In both cases, a positive value indicates positive correlation with *sudden* fractures, whereas a negative values indicates positive correlation with *other* fractures.

Table 2: Discriminant analysis function coefficients for determining *sudden*/*other* group membership.

Factor	Standardised discriminant function weights	Factor structure coefficients
WL_Thick	0.80	0.59
Max_Grad_5B	0.61	0.51
Avg_Grad_20A	-0.17	-0.42
Avg_Grad_20B	0.35	0.36
Max_Grad_20A	0.02	0.32

From the factor structure coefficients in Table 2, it is clear that weak layer thickness contributes the most to group separation, with thick layers selecting for *sudden* fractures. This has an intuitive explanation that thick weak layers are associated with *sudden collapse* fractures, which account for the bulk of the *sudden* fractures. It is possible that some *sudden planar* fractures may also be associated with relatively thick weak layers, although not sufficiently thick to be classified as *sudden collapse*. In view of this, it would be interesting to repeat this analysis with a data set containing a larger number of *sudden planar* fractures.

The variable with the second greatest contribution to group discrimination, maybe surprisingly, is the maximum hardness gradient up to 5 mm below the weak layer. For this variable, the absolute value for the maximum was used, so the positive value means that a greater maximum hardness gradient selects for *sudden* fractures. The average hardness gradient 20 mm below the weak layer also contributes to discrimination, although to a lesser extent. These two variables combined indicate that a stiffer substratum may favour *sudden* fractures.

Both the average gradient and the maximum gradient 20 mm above the weak layer also contribute to group separation, with factor loadings of -0.42 and 0.32 respectively (Table 2). The negative value for the average gradient is associated with the negative average gradient values above the weak layer (generally a decrease in hardness with an increase in depth); so a higher negative value still indicates that higher values are associated with *sudden* fractures. These variables relate to the generally accepted view that a stiffer layer of snow above the weak layer is important for fracture propagation (van Herwijnen and Jamieson, 2007).

The discriminant function was used to classify the weak layer/interfaces identified in the penetrometer signals into *sudden* or *other* fracture character groups. During the leave-one-out cross-validation method used in this analysis, the discriminant analysis function was built *N* times, where *N* is the number of weak layer records from the equalised data set (*N*=54). On each occasion, one record was withheld and classified using the function built without using that record. As a result, the exact coefficients for the discriminant functions built during the test would have varied slightly from those shown in Table 2.

Table 3 shows the results of the classification. 77.8% of *sudden* fractures were correctly classified and 81.5% of *other* fractures were correctly classified. The overall prediction rate was 79.6%. Classification parity was good between the two groups.

Table 3: Classification matrix for predicting fracture character from the selected penetrometer signal variables. Results in parentheses show actual numbers.

Class	*Sudden* (observed)	*Other* (observed)
Sudden (predicted)	(21) 77.8%	(6) 22.2%
Other (predicted)	(5) 18.5%	(22) 81.5%
Overall classification rate: 79.6%		

3. WEAK LAYER DETECTION

The results from the fracture character prediction scheme are encouraging, since they indicate that weak layers associated with fractures may be separated into “critical” (*sudden*) and “less critical” (*other*) categories using fairly rudimentary parameters associated with the penetrometer signals. One major limitation to this approach is that it is necessary to pre-identify the weak layers. Penetrometer signals must be analysed by an experienced operator and the portion of the signal representing the weak layer extracted accordingly. Outlined here is a framework for weak layer detection that could be used in conjunction with the fracture character prediction to provide rapid, automated identification of critical weak layers.

Floyer and Jamieson (2008) have shown a spiking deconvolution algorithm to be effective for tracing weak layers between slightly varying penetrometer profiles across a transect or grid of profiles. This method also relies on the pre-identification of the weak layer of interest, which is then traced across to other profiles. Various processing steps are employed before the signal being examined is reduced to a series of spikes representing the relative likelihood of that portion of the signal being similar to the weak layer of interest.

For weak layer detection, rather than weak layer tracing, the penetrometer signal being examined could be tested against a database of possible weak layer signal fragments (known as wavelets) using broadly the same mathematical framework. Although the database of weak layers also requires pre-identification of weak layers, once built, it could be used repeatedly without the need for constant updating.

The model outline is as follows:

a) Build weak layer database by identifying penetrometer signal wavelets associated with unstable snow conditions.
b) Collect penetrometer profile(s) in the forecast area.
c) Test each profile against all possible weak layers from the database.
d) Query the spiking deconvolution model output for signal portions (in the signal being examined) that closely match any of the critical weak layers in the database. This could be augmented using additional knowledge about the weak layer, such as its likely burial depth or type of weak layer expected (surface hoar, facets, etc…). Extract any signal fragments from the signal as weak layers to be further tested.
e) Run the extracted weak layers through the fracture character prediction model to determine whether they are likely to be associated with *sudden* or *other* fracture characters.

4. DISCUSSION

4.1 *Predicting fracture character*

The effects of substratum properties have not been as extensively investigated as slab properties. Recently, Habermann and others (2008) have shown, using simulations of static skier loading, that skier induced stress at the weak layer is greater when hard layers or crusts are found below the weak layer than when they are found above it. This result agrees with previous results from Jamieson and others (2001), who found that deep, persistent weak layers (the fracture character was not recorded, but it might be reasonable to assume that it was *sudden*) persisted for longer when the substratum was stiff;

also with field studies by Savage (2007), who noted that all large, deep avalanches in the study area were associated with very stiff substratums. However, this result was not detected in an earlier study by Schweizer and Jamieson (2003), who found that a pronounced hardness difference was important for distinguishing stable profiles from unstable profiles, but that the sign of the hardness change did not matter.

It should be noted, however, that Habermann and others' simulations involved calculating the applied stress at the weak layer; therefore it is likely that these results pertain mainly to fracture initiation. *Sudden* fracture character, on the other hand, is regarded to be more associated with fracture propagation (van Herwijnen and Jamieson, 2007). Schweizer and Camponovo (2001) suggested that fracture propagation depends on the difference in stiffness between the weak layer and both adjacent layers. van Herwijnen and Jamieson (2007) argue that an increase in the hand hardness difference between the weak layer and adjacent layers indicates a decrease in the relative modulus of the weak layer, which increases the fracture energy at the weak layer interface. Their data showed a significant correlation between high fracture propagation propensity and the hardness difference between the weak layer and the layer above; however, the correlation with the hardness difference between the weak layer and the layer below was insignificant. Therefore, current models of fracture propagation assume that the hardness of the substratum is important, although so far, data to back that claim up are lacking. The results of this study lend weight to there being a link between the substratum hardness and propensity for *sudden* fractures in compression tests.

The sample size used to formulate the fracture character prediction model was fairly small and the *sudden* fractures were predominantly associated with one weak layer, the 04-Feb-2008 surface hoar layer. As such, the model is likely to be detecting largely for *sudden collapse* fractures. More penetrometer pushes in snowpacks with *sudden planar* fractures are needed to reliably test the model's ability to predict this kind of fracture.

In the fracture character prediction method, the weak layers were pre-identified as being associated with compression test fractures. In order to formulate this method for application in the general case, where there was no prior knowledge of the weak layer, a third, *no fracture* category would be required. This could be randomly populated with signal fragments that were not associated with weak layers. It is likely that such a three-category model would not perform as well the two-category model tested in this study.

There was a strong possibility for bias when interpreting the fractures in the penetrometer profiles. Since the fracture character of the layer that was being interpreted in the penetrometer pushes was known, it is likely there was a tendency to select certain features in the penetrometer signal that were perceived to be associated with that type of fracture. In this way, the model was more likely to predict features that were actively selected during the interpretation. Since it is expected that certain types of fracture, (especially *sudden collapse* fractures), have a characteristic penetrometer signal, this bias is hard to overcome. It was limited to some extent by the constraint on varying the depth. Further improvements in the depth accuracy of the penetrometer or in assessing the depth of the fractures in compression tests would allow a tighter constraint on the depth location and further reduce this bias. Another possible way to reduce this bias would be to interpret the penetrometer signals without knowing the fracture character of the compression test failures.

4.2 *Weak layer detection*

One of the major advantages of digital penetrometers is the possibility for collecting a large number of profiles within a short space of time. While human interpretation of one penetrometer profile may be accomplished quite rapidly, interpreting a large number of profiles (say 100 or more) is a tedious and undesirable task.

The automated approach outlined above would be able to rapidly process the large amount of data associated with numerous penetrometer profiles and alert the operator to specific areas of concern. Such a method could potentially be built into a penetrometer which could be used by a less experienced operator to rapidly conduct a survey over a wide area of terrain. One example of a potential use for such an approach would be to determine whether in-bounds skier compaction had been effective for eliminating a weak layer of concern from a run.

5. CONCLUSIONS

A method for predicting the broad fracture character group (*sudden* or *other*) from penetrometer signals has been presented, based on a multivariate statistical analysis of

penetrometer signals interpreted against fracture character results from nearby compression tests. Using a leave-one-out cross-validation method, overall classification rates of approximately 80% were achieved. Weak layer thickness, maximum hardness gradient 5 mm below the weak layer and the average hardness gradient 20 mm above the weak layer contributed the most to discriminating between the two groups.

Results for the *sudden* category were almost certainly biased towards *sudden collapse* fractures, which dominated the data set used in this study. More observations are necessary to be able to distinguish between *sudden collapse* and *sudden planar* fractures in the *sudden* category, as well as between the *resistant planar*, *progressive compression* and *non-planar break* fractures within the *other* category.

A framework has been presented for combining a weak layer detection method based on spiking deconvolution with the fracture character prediction scheme. Such a combination, if properly developed and tested, could allow rapid, automated, critical weak layer detection from penetrometer profiles. If such a method is developed and gains acceptance, the usefulness (and hence proliferation) of penetrometers for avalanche forecasting could be dramatically enhanced.

6. ACKNOWLEDGEMENTS

For careful field observations, we thank Catherine Brown, Thomas Exner and Dave Gauthier. For logistical support and advice, we are grateful to the Avalanche Control Section of Glacier National Park. For financial support, we are grateful to the HeliCat Canada Association, the Canadian Avalanche Association, Mike Wiegele Helicopter Skiing, Canada West Ski Areas Association, the Natural Sciences and Engineering Research Council of Canada and the Canadian Commonwealth Scholarship Program.

7. REFERENCES

Birkeland, K. W., 2004. Comments on Using Shear Quality and Fracture Character to Improve Stability Test Interpretation, *The Avalanche Review*, 23(2).

Birkeland, K. W. and R. F. Johnson, 1999. The stuffblock snow stability test: comparability with the rutschblock, usefulness in different snow climates, and repeatability between observers, *Cold Regions Science and Technology*, 30, 115–123.

Canadian Avalanche Association, 2007. Observation guidelines and recording standards for weather, snowpack and avalanches, *Tech. rep.*, A revision of: NRCC Technical Memorandum No. 132, 78 pages.

Floyer, J. A., 2008. Layer detection and snowpack stratigraphy characterisation from digital penetrometer signals, (Ph.D. thesis), Dept. of Geoscience, University of Calgary, Calgary, Canada.

Floyer, J. A. and J. B. Jamieson, 2008. Avalanche weak layer tracing and detection in snow penetrometer profiles, Proceedings of the 4th Canadian Conference on Geohazards, Quebec City, QC, May 19-24 2008., 161–168.

Greene, E., K. W. Birkeland, K. Elder, G. Johnson, C. Landry, I. McCammon, M. Moore, D. Sharaf, C. Sterbenz, B. Tremper and K. Williams, 2004. Snow, Weather and Avalanches: Observational Guidelines for Avalanche Programs in the United States, American Avalanche Association and USDA Forest Service National Avalanche Center.

Habermann, M., J. Schweizer and B. J. Jamieson, 2008. Influence of snowpack layering on human-triggered snow slab avalanche release, *Cold Regions Science and Technology*: doi: 10.1016/j.coldregions.2008.05.003.

van Herwijnen, A. and B. Jamieson, 2005. Fracture character in compression tests, Proceedings of the International Snow Science Workshop (2004: Jackson Hole, Wyoming), 182–191.

van Herwijnen, A. and B. Jamieson, 2007. Fracture character in compression tests, *Cold Regions Science and Technology*, 47(1-2), 60–68.

Jamieson, J. B., 1999. The compression test – after 25 years, *The Avalanche Review*, 18(1), 10–12.

Jamieson, J. B., T. Geldsetzer and C. Stethem, 2001. Forecasting for deep slab avalanches, *Cold Regions Science and Technology*, 33(2-3), 275–290.

Johnson, J. B. and M. Schneebeli, 1999. Characterizing the microstructural and micromechanical properties of snow, *Cold Regions Science and Technology*, 30(1-3), 91–100.

Johnson, R. F. and K. W. Birkeland, 2002. Integrating shear quality into stability test results, Proceedings of the International Snow Science Workshop (2002: Penticton, BC), 508–513.

Mackenzie, R. and W. Payten, 2002. A portable, variable-speed, penetrometer for snow pit evaluation, Proceedings of the International Snow Science Workshop (2002: Penticton, BC), 294–300.

Manly, B. F. J., 1994. Multivariate Statistical Methods – A Primer, Chapman and Hall/CRC, 2 ed.

McClung, D. M. and P. Schaerer, 2006. The Avalanche Handbook, The Mountaineers, third edition ed., 342 pages.

Pielmeier, C. and M. Schneebeli, 2003. Stratigraphy and changes in hardness of snow measured by hand, ramsonde and snow micro penetrometer: a comparison with planar sections, *Cold Regions Science and Technology*, 37(3), 393–405.

Savage, S., 2007. Deep slab avalanche hazard forecasting and mitigation: the South Face at Big Sky ski area, Proceedings of the International Snow Science Workshop (2006: Telluride, Colorado), 483–490.

Schneebeli, M. and J. B. Johnson, 1998. A constant-speed penetrometer for high-resolution snow stratigraphy, *Annals of Glaciology*, 26, 107–111.

Schweizer, J., 2002. The rutschblock test — procedure and application in Switzerland, *The Avalanche Review*, 20(5), 14–15.

Schweizer, J. and C. Camponovo, 2001. The skier's zone of influence in triggering slab avalanches, *Annals of Glaciology*, 32, 314–320.

Schweizer, J. and J. B. Jamieson, 2003. Snowpack properties for snow profile analysis, *Cold Regions Science and Technology*, 37(3), 233–241.

Schweizer, J. and T. Wiesinger, 2001. Snow profile interpretation for stability evaluation, *Cold Regions Science and Technology*, 33(2-3), 179–188.

StatSoft, Inc., 2007. Electronic Statistics Textbook, Tulsa, OK: StatSoft.

Wilkinson, L., 1990. SYSTAT: The System for Statistics, Evanston, IL:SYSTAT, Inc.